Flexible Antenna with Microfluidics for the Quantification of Liquid Micro-Volumes

Giulio Maria Bianco*, Gaetano Marrocco‡,
*Pervasive Electromagnetics Lab, University of Rome Tor Vergata, Rome, Italy, giulio.maria.bianco@uniroma2.it
‡Pervasive Electromagnetics Lab, University of Rome Tor Vergata, Rome, Italy, gaetano.marrocco@uniroma2.it

***Abstract*—Microfluidics has been a significant technology for over a decade, particularly in medical and wearable devices. It allows for the manipulation of small amounts of fluid in a confined space and can synergize with auto-tuning microchips that are able to modify their internal capacitance to maximize power delivery to the antenna. Hence, the first prototype of an auto-tuning RFID sensor exploiting a microfluidic channel is designed, manufactured, and tested in this contribution. A small liquid volume of 1050 μL is successfully monitored by the auto-tuning sensor in a continuous way when using 155-μm- and 775-μm-thick microfluidic. The investigated technology could be used to monitor sweating in pathological conditions according to the point-of-care paradigm or estimate food degradation through smart packaging.**

***Index Terms*—Antenna design, auto-tuning, microfluidic, radiofrequency identification, wireless sensing.**

I. Introduction

Microfluidic has been standing as one of the most impactful enable technologies for more than a decade, mostly thanks to the advancements of medical and wearable devices [1]. Microfluidics channels allow for manipulating a small amount of fluid in a confined space, the scale typically of a few to hundreds of microliters, and they can be integrated into small devices for performing even complex in-loco sensing [2], usually through electrochemical sensors [3]. The adoption of microfluidics involved wireless devices in three main research paths: *i*) the development of antennas made of liquid metal, usually exploiting microfluidics to achieve spatial reconfigurability [4], [5], [6], *ii*) use of microfluidics to collect sensory data, eventually by chemical reactions [7], [8], [1], and *iii*) exploiting microfluidics to produce variations in the antenna's properties for sensing scopes [9], [10], [11].

Concerning liquid and humidity sensing, remote monitoring based on variations of antennas' properties has been extensively investigated in recent years as well, especially by means of RFID (radiofrequency identification) technologies. Several chipped [12], [13] and chipless [14], [15] solutions showed promising sensitivity but suffered from a significant reduction in antenna gain and, hence, reading distances. A peculiar kind of self-tuning RFID ICs (integrated circuits) has then been proposed to complete sensing without sacrificing the reading distances excessively [16]; indeed, such microchips can compensate for limited impedance mismatches and return a digital metric proportional to the retuning effort.

Accurate, low-cost sensors for quantifying liquid volumes in the order of microliters could be obtained by combining the microfluidics channels with auto-tuning ICs. Filter paper (or any other kind of microfluidics) can be shaped to carry the liquid onto the sensitive portion of the antenna, where the microchip can quantify the amount of liquid. The microfluidic-antenna interaction can be engineered and analyzed through electromagnetic simulations.

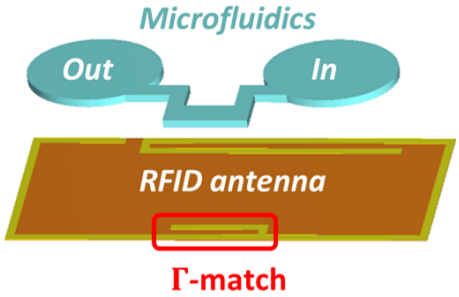

(a) Exploded view of the sensor layout, including RFID and microfluidic channel. The Γ-match is highlighted.

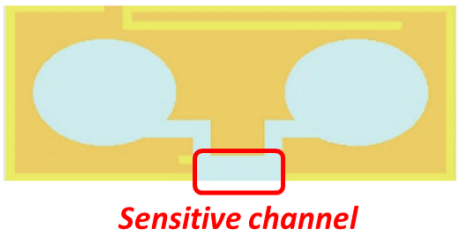

(b) View from the above of the flexible sensor. The channel constituting the sensitive part of the sensor is highlighted.

Fig. 1. Exploded and above views of the sensor layout.

The first auto-tuning RFID sensor for quantifying liquids through a paper-based microfluidic channel is here designed, prototyped, and tested. For the present proof-of-concept, a simple, straight microfluidic channel is manufactured and employed according to the sensor layout depicted in Fig. 1.

II. Background on Auto-tuning ICs

Auto-tuning microchips modify their internal capacitance to compensate for eventual impedance mismatches with the antenna and maximize the power delivered by the harvesting antenna to the IC itself [16]. Thanks to the auto-tuning, it is possible to obtain capacitive sensing without employing any capacitor in fabrication. By assuming a constant incremental

978-88-31299-09-1/24/$31.00 ©2024 IEEE

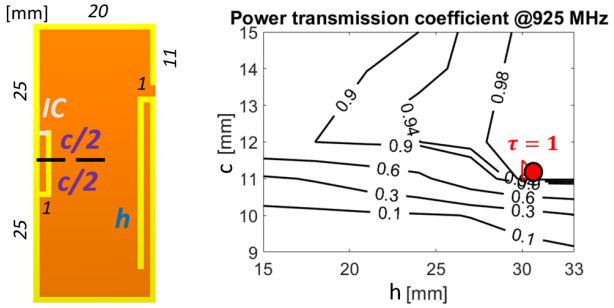

(a) Considered dipole layout.

(b) Contour chart of the power transmission coefficient with highlighted best geometry.

Fig. 2. Γ-match antenna design. The IC was accounted for by a 1-mm-wide gap.

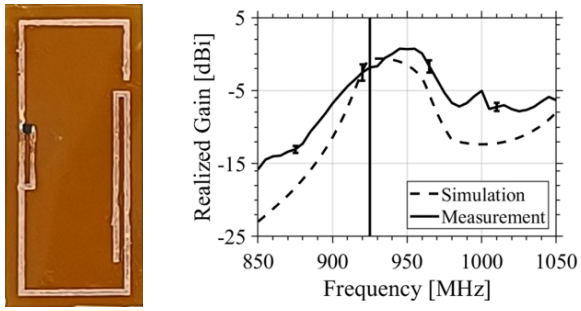

(a) Sensor prototype.

(b) Comparison between measured and simulated realized gain.

Fig. 4. Manufactured sensor prototype and its electromagnetic characterization.

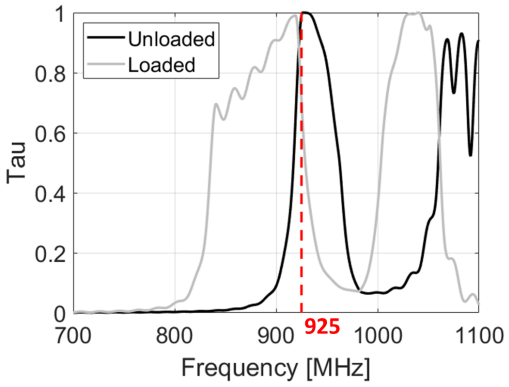

Fig. 3. Simulated τ in the absence (unloaded) and presence (loaded) of water.

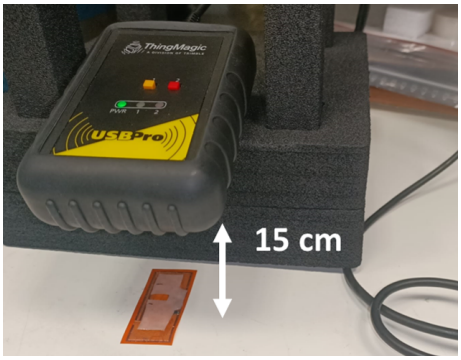

Fig. 5. Setup utilized from the sensor code measurements.

step C_s and denoting the baseline capacitance C_0, they are modelled as a conductance in parallel to the variable capacitance $C_{IC}(s)$

$$C_{IC}(s) = C_0 + sC_s, \tag{1}$$

where s is named *sensor code* (SC). The self-tuning equation determines the actual value of C_{IC} based on the frequency pulse ω and the antenna susceptance B_A

$$|\omega C_{IC}(s) + B_A| = 0. \tag{2}$$

Equation (2) is fully valid for a microchip-dependent SC range $S_{min} \leq s \leq S_{max}$. Accordingly, if the antenna susceptance is a function of a measurand Ψ (here the amount of liquid), the SC can be exploited for sensing by inverting (2) [17]:

$$s(\Psi) = \text{nint}\left\{-\frac{1}{C_s}\left[C_{IC}(S_{min}) + \frac{B_A(\Psi)}{\omega}\right]\right\}. \tag{3}$$

where nint is the nearest integer operator. Due to the auto-tuning, the power transmission coefficient τ has to be evaluated in separate ways depending on the susceptance seen by the microchip as detailed in [17].

III. Sensor Layout and Design

The sensor layout is composed of a flexible RFID antenna and a paper-based microfluidics. The selected RFID antenna layout is a Γ-match [18] dipole made by a 1-mm-wide and 35-μm-thick copper trace fixed onto a 125-μm-thick layer of Kapton (electrical characteristics at 925 MHz: dielectric constant $\varepsilon = 3.5$; loss tangent $\tan\delta = 0.0026$). The microfluidics comprises a straight channel covering the impedance adapter completely and two circular absorption and desorption pads. The Kapton was chosen as the substrate since it is flexible and easy to manufacture, whereas the Γ-match is an impedance transformer layout already experimented for the auto-tuning sensing [19]. The considered auto-tuning IC is the Magnus S3 by Axzon, having conductivity $G_{IC} = 0.482$ mS and variable capacitance in the range 1.9-2.9 pF. For the sake of simplicity, water was used as the liquid to be monitored (numerically modelled as a lossless dielectric having $\varepsilon = 78$).

The layout was optimized through parametric sweeps using the CST Microwave Studio 2023 software (hardware details follows: CPU: Intel Core i7 − 9700KF; processor frequency: 3.60 GHz; RAM: 16 GB). Fig. 2a reports the parametrized CAD of the sensor. Single-frequency simulations were performed to cut down the simulation time to about 2 minutes per simulated layout. The IC was modelled through a bidimensional port long 1 mm and its impedance, including the auto-tuning mechanism, was accounted for in postprocessing through MATLAB R2022b software.

Although both conductance and susceptance are functions

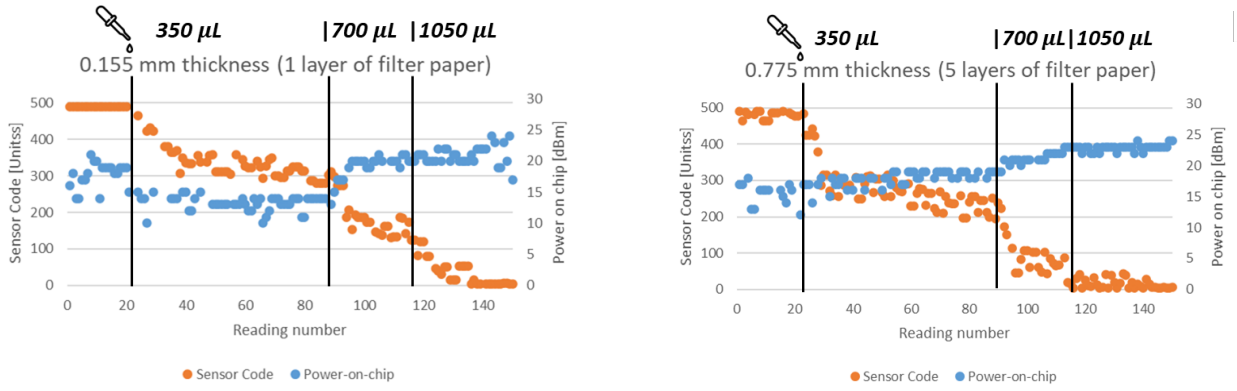

(a) Measurements with single-layer microfluidics.

(b) Measurements with five-layers microfluidics.

Fig. 6. SC measurements when microfluidics channels having different thicknesses are wet by three drops of water (350 μL).

of c and h, the length of the impedance adapter (c) dominates the susceptance seen by the IC, whilst the dipole's length (h) governs the conductance by unbalancing the length of the dipole's arms. The power transmission coefficient τ was tuned to match the highest capacitance ($C_{IC} = 2.9$ pF) since, given that the dipole works in resonance and the dielectric material lowers the resonance frequency, the returned SC is expected to lower with the water progression, as already experienced in previous works [16]. The admittance matching chart in Fig. 2b shows the parameters' values considered hereafter that guarantee unitary τ in the absence of water. The simulated τ shows a degradation of about ~ 3 dB at the working frequency due to a downward frequency shift caused by the contacting dielectric (Fig. 3).

IV. Experimental Investigation

A. Prototype Manufacturing

One dipole trace was manufactured using the milling machine 4MILL300 ATC (by Mipec [20]) and then transferred via adhesive paper onto a Kapton film as in the numerical simulations (Fig. 4a). The IC was soldered to the antenna, and the microfluidic was manually cut from sheets of filter paper Whatman grade 2 (by Zenpore [21]) whose thickness is 155 μm. The filter paper was utilized given that it is an effective and low-cost material for manufacturing simple microfluidic channels [22]. The sensitive part of the sensor is given by the "sensitive channel", which is the microfluidic channel superimposed on the Γ-adapter to contact the antenna and affect its admittance (see again the scheme of the sensor in Fig. 1b). In order to test different microfluidic thicknesses, multiple paper layers were placed one onto another, as detailed in the next subsection. The filter paper was cut manually to create the microfluidic circuit.

B. Measurements

Firstly, the electromagnetic performance in the absence of liquid was tested. The realized gain was measured through a Tagformance station (by Voyantic; linearly-polarized interrogation antenna AN-FF-WB; 55 cm of interrogation distance).

TABLE I
Sensing test of the microfluidic RFID label.

	Single-layer		Five layers	
Liquid [μL]	**SC**	**P_{oc}**	**SC**	**P_{oc}**
0	498 ± 1	18 ± 2	475 ± 19	11 ± 8
350	324 ± 46	11 ± 6	264 ± 49	14 ± 8
700	147 ± 34	19 ± 6	62 ± 33	20 ± 6
1050	21 ± 20	20 ± 4	14 ± 12	23 ± 1

Low standard deviations over 5 consecutive measurements and good agreement with simulations were observed, with an upward frequency shift mainly caused by the simplified modelling of the auto-tuning mechanism (Fig. 4b).

Afterwards, the sensing capability of the prototypes was assessed through a USB Pro reader (internal antenna; by ThingMagic) and custom software (from previous works [16]) for the retrieval of the SC and the power-on-chip (P_{oc}), which is a digital metric comprised in the range $0-32$ proportional to the power actually transferred by the RFID antenna to the IC. The distance between the dipole and the prototype was fixed to 15 cm (Fig. 5). The paper microfluidic was placed onto the RFID tag properly, and two different thicknesses were tested by using 1 and 5 layers to experimentally investigate how the increased thickness can affect the antenna response [23]. Liquid quantity was manually increased by using a micropipette (M1000 by QWork) by incremental steps of about ~ 350 μL.

Fig. 6 depicts the temporal tracks recorded during measurements, including both the SC and the P_{oc}. As expected, when the liquid inserted in the absorption pad increases, the SC lowers. The sensor exploits a broad range of SC values ranging from the upper to lower saturation (from 500 to 10 units, approximatively) and achieves a sensitivity of $S \simeq \Delta s/\Delta m g_{H_2O} = 490/1050\ mg^{-1}_{H_2O} = 0.46\ mg^{-1}_{H_2O}$, i.e., about 1 SC unit every 2 mg of water. The P_{oc} increased during the experiments; although simulations predicted a lowering τ (Fig. 3), the frequency shift between the simulated and measured realized gain causes the maximum gain to be at a higher frequency than predicted (Fig. 4b). Thus, the presence of water causes a downward frequency shift and heightens the

gain, explaining the observation.

Different microfluidics thicknesses were lastly tested. The same quantity of water returned lower SC and higher P_{oc} values, and higher standard deviations when the microfluidic channel was thicker (Table I). The higher dispersion of data points is probably due to the imperfect positioning of the layers and/or the thin air layers between the filter paper. The lower SC and higher P_{oc} suggest that the liquid stayed longer on the sensing area when the microfluidic channel was thicker, coherently with [23]. Overall, the liquid quantity was successfully digitalized and monitored by the auto-tuning sensor, even though calibration is generally necessary to account for the microfluidic thickness, eventually by numerical simulations.

V. Conclusion

In this contribution, the first flexible, auto-tuning RFID tag for quantifying liquids by exploiting a microfluidic channel was designed, prototyped, and experimentally tested. The antenna geometry is a Γ-match returning maximum power transfer coefficient, and up to 1050-μL were continuously monitored by the sensor using low-cost paper-based microfluidic with two different thicknesses. The sensitivity of the tested layout is about 1 SC unit every 2 mg of water.

Several applications would then benefit from such sensors, for instance, in the fields of medical points-of-care (PoCs) [24] and food quality monitoring. Such an RFID could monitor sweating in pathological conditions like hyperidrosis [25], or it could be integrated into smart packaging to estimate food degradation thanks to the (eventually "freeze-thaw") "drip loss" [26], [27], [28] in order to minimize food waste.

The following open issues should be addressed in future research. The effects of the microfluidic channel thickness have not been accounted for during the antenna design, which was performed in unloaded (i.e., without any liquid) conditions. Moreover, the raw SC was employed to investigate the sensor, while better accuracy is expected when processing data properly. Then, the layout proposed here should be investigated further to apply the antenna-microfluidic system to the healthcare and food sectors as envisaged in the Introduction, and a direct performance comparison in actual use scenarios with the existing literature has to be completed.

Acknowledgment

Work supported by Project ECS 0000024 Rome Technopole, CUP B83C22002820006, NRP Mission 4 Component 2 Investment 1.5, Funded by the European Union – NextGenerationEU. Spokes and Flagships: Spoke 2, project "Eco-friendly Electronic Labels for Food and Plastic Waste" (Flagship Project 3); and Spoke 1, project: "Next-gen Point of Cares: Chemical-Physical Sensors with Wireless Interface for Health Monitoring in Domestic Settings" (Flagship Project 7).

References

[1] G. Chen, J. Zheng, L. Liu, and L. Xu, "Application of microfluidics in wearable devices," *Small Methods*, vol. 3, no. 12, 2019.

[2] S. Li, Z. Ma, Z. Cao, L. Pan, and Y. Shi, "Advanced wearable microfluidic sensors for healthcare monitoring," *Small*, vol. 16, no. 9, 2020.

[3] P. Khashayar, S. Al-Madhagi, M. Azimzadeh, V. Scognamiglio, and F. Arduini, "New frontiers in microfluidics devices for miRNA analysis," *TrAC - Trends in Analytical Chemistry*, vol. 156, 2022.

[4] J. Ren and X. Yang, "Design of frequency reconfigurable antenna based on liquid metal," *Lecture Notes on Data Engineering and Communications Technologies*, vol. 153, p. 1274 – 1281, 2023.

[5] B. Mohamadzade, R. B. V. B. Simorangkir, S. Maric, A. Lalbakhsh, K. P. Esselle, and R. M. Hashmi, "Recent developments and state of the art in flexible and conformal reconfigurable antennas," *Electronics (Switzerland)*, vol. 9, no. 9, p. 1 – 26, 2020.

[6] K. N. Paracha, A. D. Butt, A. S. Alghamdi, S. A. Babale, and P. J. Soh, "Liquid metal antennas: Materials, fabrication and applications," *Sensors*, vol. 20, no. 1, 2020.

[7] L. Fiore *et al.*, "Microfluidic paper-based wearable electrochemical biosensor for reliable cortisol detection in sweat," *Sensors and Actuators B: Chemical*, vol. 379, p. 133258, 2023.

[8] A. Riente, G. M. Bianco, L. Fiore, F. Arduini, G. Marrocco, and C. Occhiuzzi, "An RFID sensor with microfluidic for monitoring the pH of sweat during sport activity," in *2023 17th European Conference on Antennas and Propagation (EuCAP)*, 2023, pp. 1–4.

[9] L. Zhu, N. Alsaab, M. M.-C. Cheng, and P.-Y. Chen, "A zero-power ubiquitous wireless liquid-level sensor based on microfluidic-integrated microstrip antenna," *IEEE Journal of Radio Frequency Identification*, vol. 4, no. 3, p. 265 – 274, 2020.

[10] Y. Seo, M. U. Memon, and S. Lim, "Microfluidic eighth-mode substrate-integrated-waveguide antenna for compact ethanol chemical sensor application," *IEEE Transactions on Antennas and Propagation*, vol. 64, no. 7, p. 3218 – 3222, 2016.

[11] C. Mariotti, W. Su, B. S. Cook, L. Roselli, and M. M. Tentzeris, "Development of low cost, wireless, inkjet printed microfluidic RF systems and devices for sensing or tunable electronics," *IEEE Sensors Journal*, vol. 15, no. 6, p. 3156 – 3163, 2015.

[12] M. A. S. Tajin, W. M. Mongan, and K. R. Dandekar, "Passive RFID-based diaper moisture sensor," *IEEE Sensors Journal*, vol. 21, no. 2, pp. 1665–1674, 2021.

[13] X. Chen, H. He, Z. Khan, L. Sydänheimo, L. Ukkonen, and J. Virkki, "Textile-based batteryless moisture sensor," *IEEE Antennas and Wireless Propagation Letters*, vol. 19, no. 1, pp. 198–202, 2020.

[14] Y. Xue, B. Hou, S. Wang, Y. Shang, B. Chen, and Y. Ju, "A highly sensitive paper-based chipless RFID humidity sensor based on graphene oxide," *Sensors and Actuators A: Physical*, vol. 358, 2023.

[15] G. Marchi, V. Mulloni, F. Acerbi, M. Donelli, and L. Lorenzelli, "Tailoring the performance of a nafion 117 humidity chipless RFID sensor: The choice of the substrate," *Sensors*, vol. 23, no. 3, 2023.

[16] G. M. Bianco, S. Amendola, and G. Marrocco, "Near-field constrained design for self-tuning UHF-RFID antennas," *IEEE Transactions on Antennas and Propagation*, vol. 68, no. 10, p. 6906 – 6911, 2020.

[17] F. Naccarata, G. M. Bianco, and G. Marrocco, "Sensing performance of multi-channel RFID-based finger augmentation devices for tactile internet," *IEEE Journal of Radio Frequency Identification*, vol. 6, p. 209 – 217, 2022.

[18] C. Balanis, *Antenna Theory: Analysis and Design*, 2005.

[19] F. Naccarata, M. Di Cristofano, and G. Marrocco, "RFID-based endoleak detection by dissolvable antennas and auto-tuning IC," 2023.

[20] Mipec, ''PCB milling machine 4MILL300ATC - automatic tool change," 2023. [Online.] Available.

[21] Zenpore, ''Filter paper standard grade 2," 2023. [Online.].

[22] W. Li, X. Ma, Y.-C. Yong, G. Liu, and Z. Yang, "Review of paper-based microfluidic analytical devices for in-field testing of pathogens," *Analytica Chimica Acta*, vol. 1278, 2023.

[23] H. Bruus, ''Poiseulle Flow," in Theoretical Microfluidics, 3rd ed., Oxford, United Kingdom: Oxford University Press, 2016, ch. 4, sec. 4, pp. 19-42. [Online.] Available.

[24] S. Mondal, N. Zehra, A. Choudhury, and P. K. Iyer, "Wearable sensing devices for point of care diagnostics," *ACS Applied Bio Materials*, vol. 4, no. 1, p. 47 – 70, 2021.

[25] H. W. Walling and B. L. Swick, "Treatment options for hyperhidrosis," *American Journal of Clinical Dermatology*, vol. 12, no. 5, p. 285 – 295, 2011.

[26] K. Manheem *et al.*, "A comparative study on changes in protein, lipid and meat-quality attributes of camel meat, beef and sheep meat (mutton) during refrigerated storage," *Animals*, vol. 13, no. 5, 2023.
[27] Y. Huang, M. Zhang, and P. Pattarapon, "Reducing freeze-thaw drip loss of mixed vegetable gel by 3d printing porosity," *Innovative Food Science and Emerging Technologies*, vol. 75, 2022.
[28] N. Nakazawa and E. Okazaki, "Recent research on factors influencing the quality of frozen seafood," *Fisheries Science*, vol. 86, no. 2, p. 231 – 244, 2020.